


 Cite this: *RSC Adv.*, 2024, 14, 11694

# Immunomodulatory zymosan/ $\iota$ -carrageenan/agarose hydrogel for targeting M2 to M1 macrophages (antitumoral)<sup>†</sup>

 Geetha Venkatachalam,<sup>a</sup> Jayant Giri,<sup>b</sup> Saurav Mallik,<sup>c</sup> Gandarvakottai Senthilkumar Arumugam,<sup>a</sup> Manavalan Arulmani,<sup>d</sup> Vimal Kumar Dewangan,<sup>e</sup> Mukesh Doble<sup>ib</sup>\*<sup>d</sup> and Zhongming Zhao<sup>\*f</sup>

Several studies have been performed on the immunomodulatory effects of yeast  $\beta$ -(1,3) glucan, but there is no proper evaluation of the thermal and immunomodulating properties of zymosan (ZM). Thermogravimetry analysis indicated a 54% weight loss of ZM at 270 °C. Circular dichroism showed absorption peaks in the region of 250 to 400 nm, suggesting a helical coil  $\beta$ -sheet configuration. XRD showed a broad peak at  $2\theta$  of 20.38°, indicating the crystalline nature, and the size was found to be 23 nm. ZM is biocompatible and showed no toxicity against L929 and RAW 264.7 cell lines (cell viability > 90%). Immunomodulatory studies with PCR showed upregulation of M1 genes in human differentiated THP-1 macrophage cell lines, which were responsible for antitumor properties. The uptake of ZM particles inside the differentiated THP-1 macrophages and Raw 264.7 cells was confirmed (Video clip<sup>†</sup>). ZM particle uptake *via* Dectin-1 was identified by competitive receptor blocking. Seaweed derived carrageenan/ZM/agarose hydrogel was successfully prepared (@5 : 5 wt%) and was seen to support the growth of L929 cells ( $1 \times 10^5$  cells per mL) and have a higher swelling ( $\approx 250$ –280%). This study indicates that ZM-based hydrogel could be a potential drug carrier (Rifampicin and Levofloxacin) for targeting tumour-associated macrophages (M2).

 Received 13th October 2023  
 Accepted 1st April 2024

DOI: 10.1039/d3ra06978h

[rsc.li/rsc-advances](https://rsc.li/rsc-advances)

## 1. Introduction

Zymosan (ZM), an immunomodulatory polysaccharide, is insoluble and highly branched  $\beta$ -(1,3)-glucan produced from *Saccharomyces cerevisiae*. Yeast contains  $\beta$ -(1,3,1,6) glucan and mannoproteins in the outer layer, whereas the chitin and nucleic acids is present in the inner layer.<sup>1</sup> These high molecular weight non-digestible glucans are used as dietary fibers and functional foods, and also exhibit antitumor, anti-inflammatory, anti-hypercholesterolemia, and anti-hyperglycaemia activities.<sup>2</sup> In our previous research, solubility of high molecular weight ZM is enhanced by a two-step amination process which resulted in a product which was characterised (structural prediction by 2D

NMR) with molecular weight of 296 kDa (MALDI-MS MS). Most of the immunomodulatory polysaccharides have been used for different applications including drug carrier, siRNA delivery vehicle, hydrogel, scaffolds, biosensors, electro conductive, food additives, nutraceuticals, and cosmetics and wound healing patches but there is no study on thermal and immunomodulatory properties of ZM. The current work deals with these aspects.

$\beta$ -Glucan is a  $\beta$ -D-glucopyranose polymer that has a linear chain linked by  $\beta$ -1,3 or  $\beta$ -1,4 glycosidic bonds and has -1,6 side chains. Mostly present in yeast, fungi, bacteria, seaweeds, and grains (oats and barley). Immuno-modulating activity of  $\beta$ -glucans varies depending on the degree of branching, tertiary structure, purity, solubility, conformation in the solution, molecular weight, and charge. ZM are recognized by the Dectin-1 and complement receptor-3 (CR3) of the immune cells which includes dendritic, macrophages, and neutrophils and activates both innate and acquired immunity. Direct stimulation of the collagen biosynthesis in fibroblast cells is achieved by  $\beta$ -glucan receptors on human dermal fibroblasts.

$\beta$ -Glucans based polysaccharides like ZM, curdlan, fungal glucan, lentinan, are essential to combat inflammation and boost the immune system and has no flavor, color, taste or odor and forms aqueous suspension in water and soluble in acid or alkali. Most pro-inflammatory cytokines like TNF $\alpha$ , IL-1 $\beta$ , and IL-6 are elevated during prolonged inflammation whereas the anti-inflammatory cytokines like TGF- $\beta$  and IL-10 are

<sup>a</sup>Bioengineering and Drug Design Lab, Department of Biotechnology, Indian Institute of Technology Madras, 600036, Chennai, Tamilnadu, India

<sup>b</sup>Department of Mechanical Engineering, Yeshwantrao Chavan College of Engineering Nagpur, India

<sup>c</sup>Department of Pharmacology and Toxicology, University of Arizona, Tucson, AZ, USA

<sup>d</sup>Department of Cariology, Saveetha Dental College, SIMATS, 600077, Chennai, Tamilnadu, India. E-mail: mukeshdoble.sdc@saveetha.com; mukeshd@iitm.ac.in

<sup>e</sup>Department of Metallurgical and Materials Engineering, Indian Institute of Technology Madras, 600036, Chennai, India

<sup>f</sup>McWilliams School of Biomedical Informatics, The University of Texas Health Science Center at Houston, Houston, TX, USA. E-mail: Zhongming.zhao@uth.tmc.edu

<sup>†</sup> Electronic supplementary information (ESI) available. See DOI: <https://doi.org/10.1039/d3ra06978h>


downregulated in diabetic wounds and other infectious diseases. Recent research had shown that the co-transfer of mannan/ $\beta$ -1,6-glucan-containing polysaccharides (induced  $\text{iTreg}$  cells) which efficiently prevents the colitis and experimental autoimmune encephalomyelitis (EAE). Structural specificities of cell surface  $\beta$ -glucan polysaccharides regulate commensal yeast mediated immune-modulatory activities.

Zymosan had shown the ability to protect and deliver drugs, adjuvants, single strand DNA and in the adsorption of toxins. ZM is chosen for this study, because it has the ability to enter inside cells *via* the Dectin-1 receptor, which can be seen in the Video abstract.<sup>†</sup> Glucans could exist in many conformations, such as single helix, double helix, triple helix, random helix, worm-like shapes, rod and aggregation. Macrophages are the major phagocytic cells of our immune system. Mainly the tumour associated macrophages (TAMs) are major therapeutic targets because these cells contribute to the inflammatory component in stroma of tumors. Tuberculosis is caused by *Mycobacterium tuberculosis*, the bacterium resides inside the macrophages and causes tuberculosis, Tb affects one third of the global population. Tumor associated macrophages (TAMs) are involved in spinal tuberculosis which is also caused by *Mycobacterium* results in the formation of cancer and tumors. In this case, macrophage act as host for *M. tuberculosis* hence targeting this with ZM based drug delivery through receptor mediated is best strategy to achieve high therapeutic efficacy. Targeting cancer cells is challenging and most of the anticancer drugs used are showing low response rates at reaching target cells. Recently many approaches have been used to treat cancer cells, here the ZM used as target to macrophage and it showed upregulation of M1 phenotype and blocks M2 (pro-tumoral) formation, thus it would be an efficient candidate for cancer therapy and wound healing.

M1 genes are expressed from macrophages upon stimulation of microbial products or interferons- $\gamma$ . M1 macrophages are potent effector cells which produce cytokines and effectively kill tumour cells and microorganisms.<sup>3</sup> Plasticity and diversity of macrophages display their forms as M1 and M2 polarized states. TAMs display M2 features which are pro-tumoral whereas M1 expresses antitumour features. Tumour progression, metastasis and recurrence after treatment are majorly governed by TAMs, and it is known that reprogramming the TAMs to M1 like macrophages (antitumoral) would lead to tumour regression. Generally these procedures are achieved through immunotherapy, chemotherapy and radiotherapy.<sup>4</sup> ZM could bind to the macrophages through Dectin 1 receptors (and initiate cytokine and chemokine production) which enhance the M1 like macrophages and repress the M2 forms which ultimately prevents TAMs. TNF $\alpha$  and CXCL10 are M1 macrophage marker genes. The M2 macrophages (Marker genes IL 10, CCL18, CCL22) promotes tumour development So blocking M2 expression and activating the M1 phenotype through treatment with ZM could be a novel approach to target TAMs.

Hydrogels are made as useful functional materials which are chemically or physically cross linked polymer networks. Hydrogels are made from synthetic polymers like, poly(*N*-isopropyl acrylamide), poly(vinyl alcohol), poly(2-acrylamido-2-methylpropanesulfonic acid), poly(acrylic acid) or natural

polysaccharides like curdlan, beta glucan (*Pleurotus ostreatus*), schizophyllan, paramylon, scleroglucan, grifolan and proteins, peptides and polyesters. Polysaccharides of microbial sources are highly preferable because of its high production, unique properties and biocompatibility. Chitosan, agarose, and alginate have been widely used in biomedical engineering applications. In order to improve the immunomodulatory effects of ZM, a hydrogel of ZM (immunomodulator)/carrageenan (antitumour)/agarose (gelling agent) was made by physical crosslinking. Blending carrageenan (cationic), ZM (anionic) with agarose initiates hydrogel formation by interacting with neutral charged agarose. Iris moss is a jelly like substance, broadly useful, emulsifier, provides gelation and viscosity. Mostly  $\iota$  carrageenans form three-dimensional gels (no syneresis), freeze/thaw stable when compared with kappa ( $\kappa$ ), lambda ( $\lambda$ ), mu ( $\mu$ ), nu ( $\nu$ ), and theta ( $\theta$ ) carrageenans.

$\iota$ -Carrageenan derived from marine red algae (*Rhodophyceae*) a anionic sulphated polygalacton ( $\alpha$ -(1,3)  $\text{D}$ -galactose) and  $\beta$ -(1,4)-(3,6)-anhydro-galactose (3,6-AG) with 15–40% of ester sulphates.<sup>5,6</sup> Agarose an seaweed and inexpensive biopolymer widely used as gelling agent, thickener and stabilizer which is composed of  $\text{D}$ -galactose and 3,6-anhydro  $\text{L}$ -galactopyranose units. In aqueous solution agarose forms fibrous network with  $\iota$ -carrageenan without adding any crosslinkers.<sup>7</sup> Agarose is biocompatible, biodegradable and enhances the stability and swelling properties of biopolymer based hydrogels.<sup>8</sup>

The thermal analysis, structural properties like circular dichroism, XRD, and expression of M1, M2 and TLR-2 genes after incubating the cells with ZM and their uptake by differentiated THP-1 macrophage cells were evaluated. A hydrogel was made using ZM and  $\iota$ -carrageenan, a derived biopolymer. The hydrogel supports the growth of L929 fibroblast cell lines. The aim of this work is to characterize the properties, biological, immunomodulatory effects of ZM on M1 and M2 marker genes, further ZM hydrogel preparation along with carrageenan and agarose (reported for several beneficial biological properties). The hydrogel could play a dual role as tumor targeting and also as wound healing material.

## 2. Experimental details

### 2.1 Materials

Methanol (SRL laboratories), rhodamine B, DMEM and other chemicals are from Himedia Laboratories Pvt. Ltd. ZM (*Saccharomyces cerevisiae*), Gene primers TNF $\alpha$ , CXCL10, IL10, CCL18, CCL22, TLR2 from Merck Sigma Aldrich India. Fetal Bovine Serum (Gibco, Origin-South America). Human THP-1, RAW 264.7 macrophage and L929 fibroblast cells were purchased from National Centre for Cell sciences (NCCS), Pune.

### 2.2 Analytical measurements

TGA7, PerkinElmer, Q500 Hi-Res TGA7 from TA instruments were used for the determination of thermal stability of ZM. Aluminum oxide crucible were used to place the sample of 1.06 mg and then heated at 30 to 830  $^{\circ}\text{C}$  at a rate of 20  $^{\circ}\text{C min}^{-1}$  under nitrogen atmosphere (at a flow rate of 80  $\text{mL min}^{-1}$ ).<sup>1</sup> Secondary structural



changes of the ZM were monitored using Jasco J-810 spectropolarimeter (Easton, MD). 2 mg of ZM were used to record UV-CD spectra. A wavelength range of 200–600 nm using a 10 mm path length cuvette at room temperature. Scanning was performed at 100 nm min<sup>-1</sup> with a 2 nm bandwidth for three times, baseline spectra were carried out with aqueous solution.<sup>9</sup> Fine powdered sample of ZM (500 mg) Powder X-ray was performed at room temperature on the Powder x-ray was performed with fine powdered sample of ZM (500 mg) at room temperature on the Powder x-ray diffractometer (structure determination with phase analysis using Cu K $\alpha$  radiation). Data were scanned with wide angle lynx eye detector of high speed for fast collection by small angle scan ( $2\theta = 0.5^\circ$ ). Data were evaluated by HighScore plus software package.<sup>10</sup>

### 2.3 Cell viability of ZM against L929 and RAW 264.7

ZM powdered particle morphology was viewed by scanning electron microscope (FEI Quanta FEG 200-High Resolution). 2 mg of homogeneous preparation of ZM were analysed for its particle size distribution in Zetatract-zeta potential particle size analyzer (Microtrac Inc.). The cell viability of the ZM was carried out by MTT [3-(4,5-dimethylthiazole-2-yl) 2,5-diphenyl tetrazolium bromide] assay. RAW 264.7 cell lines and L929 a murine fibroblast (NCCS, Pune) were used for testing the polymer cytotoxicity on cells. L929 and RAW 264.7 cells with concentration of 10<sup>-4</sup> cells mL<sup>-1</sup> were seeded on DMEM for 24 h in 96 well plates and incubated at 5% CO<sub>2</sub>. Different concentrations of ZM (10–100  $\mu\text{g mL}^{-2}$ ) added to the cells and kept for 24 h incubation. Further MTT (5 mg mL<sup>-1</sup>) was added to 96 wells and incubated for 4 h. Formazan crystals were formed which is solubilized with 100  $\mu\text{l}$  of DMSO. The absorbance was read at 570 nm Bio-Rad, Richmond Microplate reader (California).

### 2.4 ZM uptake by differentiated THP-1 and Raw 264.7 macrophage

The rhodamine B-tagged (Rho B-tagged) ZM were produced by previously mentioned method.<sup>1</sup> Differentiated THP-1 macrophages and Raw 264.7, 1  $\times$  10<sup>5</sup> cells per mL incubated separately with Rho B-tagged particles for 4 h. After incubation the cells were washed thrice with PBS to remove unattached particles. The cells were fixed with 5% paraformaldehyde (20 min at 37  $^\circ\text{C}$ ) and washed with PBS. Then 3  $\mu\text{l}$  of DAPI (4',6-diamidino-2-phenylindole) a nuclear dye was added and the THP-1 cells were viewed under Olympus BX51 fluorescence microscope (Olympus America Inc., USA) whereas the stained Raw 264.7 were visualized under Nikon confocal microscope A1HD25. Simultaneously the Rho B-tagged THP-1 macrophages cells were lysed with lysis buffer and centrifuged for 13 000 rpm for 10 minutes. The supernatant were used for measuring the fluorescence at 540 nm excitation and 575 nm emission by using PerkinElmer EnSpire microplate reader, Singapore.

### 2.5 ZM uptake by raw 264.7 cells – Video clip

Raw 264.7 cells with a concentration of 1  $\times$  10<sup>5</sup> cells per mL were grown in 6 well plate and treated 100  $\mu\text{g mL}^{-1}$  of Rho B-tagged ZM particles for 4 h in a CO<sub>2</sub> incubator. To check the

particle uptake by the cells it was directly viewed under the Olympus Magcam DC 10 Microscopy. After 3 h the cells were viewed and video was taken.

### 2.6 Competitive receptor blocking

Raw 264.7 cells (2  $\times$  10<sup>5</sup> cells per mL) grown on 24 well plate, added with 100  $\mu\text{g mL}^{-1}$  of methyl- $\beta$ -CD (M- $\beta$ -CD), curdlan and sucrose separately and incubated for 1 h and then treated with 100  $\mu\text{g mL}^{-1}$  of Rho B-tagged particles and incubated for 3 h. After incubation Raw 264.7 cells were washed thrice with PBS further lysed by lysis buffer to quantify the uptake of Rho B-tagged ZM particles. The supernatant were measured for its fluorescence intensity excitation at 540 nm and emission at 575 nm using a microplate reader (EnSpire, PerkinElmer, Singapore).

### 2.7 M1 and M2 gene expression by ZM on differentiated THP-1 macrophage cells

THP-1 monocytes 1  $\times$  10<sup>5</sup> cells per mL cultured in 6 well plate with RPMI medium for overnight and the cells were differentiated with macrophage like cells using 30 nM phorbol myristate acetate (PMA) for 24 h. The differentiated cells then added with 1 mg of ZM, 10  $\mu\text{g mL}^{-1}$  of lipopolysaccharide act as positive control (induce inflammatory response). Cells without LPS treatment act as control. Incubated for 6 h and the cells washed twice with PBS to remove the unattached particles. RNA iso Plus (Total RNA extraction reagent, Takara Bio Inc., Japan) were used for RNA isolation from the cells. Reverse transcription (1  $\mu\text{g}$  of RNA) was carried out using a cDNA Reverse transcription Kit (Applied biosystems, Thermo Fischer Scientific, USA). The M1 (marker genes TNF $\alpha$  and CXCL10), M2 (marker genes IL 10, CCL18, CCL22) and TLR2 gene (Table. S1 $\dagger$ ) expression was analyzed by SYBR Premix Ex Taq II kit (Takara Bio, USA) and the expression is normalized with respect to the Gapdh and the fold change was determined by  $\Delta\Delta\text{Ct}$  method.<sup>11</sup>

### 2.8 Preparation of ZM/ $\iota$ -carrageenan hydrogel without cross linker

$\iota$ -Carrageenan were used for making hydrogel along with immunomodulatory ZM as a copolymer. To prepare a stable, soft gel the ZM (beta (1,3)-glucan) an anionic and  $\iota$ -carrageenan a cationic polymer were used without cross linkers. ZM/ $\iota$ -carrageenan ratios (wt%) were 10 : 0 (C1), 9 : 1 (C2), 5 : 5 (C3). ZM was hydrated using distilled water to obtain a homogeneous suspension<sup>12</sup> and then heated at 80  $^\circ\text{C}$  for 1 h and added with  $\iota$ -carrageenan and clearly suspended in deionized water and stirred for overnight to obtain a homogeneous mix. To achieve a clear, narrow, small sized gel (11 mm depth and 5 mm diameter) the polymeric gel solution were poured onto a 96 well plate. Well plate were kept for 12 h incubation to set the hydrogel.<sup>12</sup> To obtain a porous gel for better cell growth the wet hydrogel were lyophilized by Larker Lyophilizer.

### 2.9 ZM/ $\iota$ -carrageenan/agarose hydrogel

The properties of different ratios of hydrogels C1, C2, C3 were depicted in Table. S2. $\dagger$  Among the different ratios of hydrogel, the C1 and C2 had poor strength and not stable whereas the C3 (ZM/I



5:5 wt%) showed stable gel but the freeze dried gels were dispersed and cannot support cell growth after placing in a cell culture media. To enhance its stability a gelling agent agarose was added which enhances the stability and rigidness of ZM and ι-carrageenan. ZM and ι-carrageenan (5:5 wt%) was clearly suspended in deionized water for overnight, a clear suspension of both the polymers were obtained after 24 h in magnetic stirrer, then 0.4% agarose were added to the above suspension and mixed well for 5 minutes. Finally the suspension was poured onto 96 well plate to obtain a well formed hydrogel. To obtain a porous network of gel, the hydrogels were freeze dried and used. The stable gels were placed in 6 well plate in DMEM and L929 cells of  $1 \times 10^5$  cells per mL were seeded on the gel and kept incubation for 48 h.<sup>12</sup> The growth of the cells on the hydrogel was monitored by Olympus light microscopy. Then the hydrogels along with cells were fixed by ethanol gradient fixation and viewed under a Scanning Electron Microscopy (FEI Quanta FEG 200-High Resolution).

### 2.10 Swelling of the ZM/ι-carrageenan/agarose hydrogel

To study the swelling effect of the dry hydrogels, the  $1 \times 1 \text{ cm}^2$  hydrogels were placed in 10 mL of phosphate buffered saline (PBS) with a pH of 7.4 inside the test tubes and kept at 37 °C. The hydrogels were taken at different time intervals, and the moisture on the hydrogel was absorbed by filter paper and weighed. After drying, the percentage of swelling was measured as a function of time by using the following equation:

$$\text{Swelling}(\%) = \frac{(W_t - W_i)}{W_i} \times 100$$

where, initial ( $W_i$ ) and final dry weight ( $W_t$ ) of the hydrogels at different time intervals.

### 2.11 *In vitro* degradation of the ZM/ι-carrageenan/agarose hydrogel

The degradation of the hydrogel was evaluated in *in vitro* by immersing the  $1 \times 1 \text{ cm}^2$  samples in PBS inside falcon tubes at 37 °C for 15 days. The hydrogels were taken at different time intervals, washed with distilled water, and dried, and their weight was quantified at each point. The percentage weight loss equation.

$$\text{Weight loss}(\%) = \frac{(W_t - W_i)}{W_i} \times 100$$

where, initial ( $W_i$ ) and final dry weight ( $W_t$ ) of the hydrogels respectively at different time points.

### 2.12 Statistical analysis

Graph PadPrism (version 6.0) were used, one-way and two-way ANOVA were used. All values were expressed as the mean  $\pm$  standard deviation.

## 3. Results and discussion

### 3.1 Characterization of ZM by TGA, XRD and CD

Thermogravimetric analysis shows the degradation pattern of ZM in three different temperatures. Initial weight loss of

9.174% was observed at 100 to 270 °C. A sharp major weight reduction was observed at 270 to 390 °C which is 52.03%. The final weight reduction of 33.64% was observed between 330 to 700 °C (Fig. S1†). There is no residual polymer in TGA which represents the complete degradation of ZM. The similar TGA weight loss pattern was observed with baker's dry yeast which is  $\sim 65\%$  at 650 °C and brewing yeast was  $\sim 65.3\%$  at 155–450 °C.<sup>13</sup> The strongest peak was observed at 20.38° which are in agreement with the literature values reported for films of yeast glucan.<sup>10</sup> ZM XRD spectra broad peaks demonstrate that the ZM was a compound of well crystalline nature (Fig. 1A). Using Debye Scherrer formula the grain size of ZM was estimated to be approximately 23 nm. It is evident that pure ι-carrageenan displays an amorphous nature as indicated by its broad peak at  $2\theta = 22.17^\circ$ . Dried agarose exhibits crystalline peaks at four ranges 19.27, 27.15, 40.90, and 53.34°, which are attributed to the ordered stacking of polysaccharide rings. Additionally, the XRD patterns of the hydrogel reveal a broad peak at 21.25°, indicating its amorphous nature. The β-1,6 glucan linkage of yeast glucan were observed with literature reports at 42.9°, it was not observed with our ZM.<sup>10</sup> From our previous reports the MALDI-TOF, <sup>1</sup>H, <sup>13</sup>C NMR showed that the ZM having degree of polymerization (DPn) above  $-1250$  and their corresponding molecular weight MW = 2–3 Lakhs showed an helix conformation. Whereas practically it behaves as a random coil, a conformational transition occurring in the region between helix to random coil as per literature Kozo Ogawa in dilute aqueous solution. Saito *et al.*, already reported the similar pattern of helix coil transition with beta glucan<sup>14</sup> as shown in Fig. 1B, the ZM exhibits two positive CD peaks at 320 nm and 450 nm in the visible region.<sup>9</sup>

### 3.2 Cell viability of ZM against L929 and RAW 264.7

In scanning electron microscopy the ZM appears (Fig. 1C) as oval shaped particles (3–5 μm in size), in aqueous solution the particle size is 3.24 to 5.71 μm (Fig. 1D). Cell viability test was carried out to check the cytotoxicity effects of polymer on cells. Both L929 fibroblast cells and RAW 264.7 were used for this experiment, because the former plays a major role in cell differentiation, wound healing, extracellular matrix remodeling and structural framework whereas the latter one is involved in phagocytic process and innate immunity. The effect of ZM on cells were tested at different concentrations (10 to 100 μg mL<sup>-1</sup>). The cell viability were measured after 24 h using MTT assay. ZM showed above 90% cell viability in both the cell lines up to 100 μg mL<sup>-1</sup> (Fig. 2) and it could be considered as nontoxic to cells according to the ISO 10993-5. No statistical significance was observed with these two treatments. These results are accordance with the already reported curdlan nanoparticles non-cytotoxic effects on L929 and RAW 264.7 cells.<sup>11</sup> *S. cerevisiae* β-glucan preparations enhanced the proliferation (above 90%), phagocytosis and cytokine production of murine macrophages and dendritic cells.<sup>15</sup> Bioactive (1-3),(1-6)-β-D-glucan of *Grifola frondosa* a edible medical mushroom, showed cell viability of above 90% in RAW264.7 macrophages.<sup>16</sup>



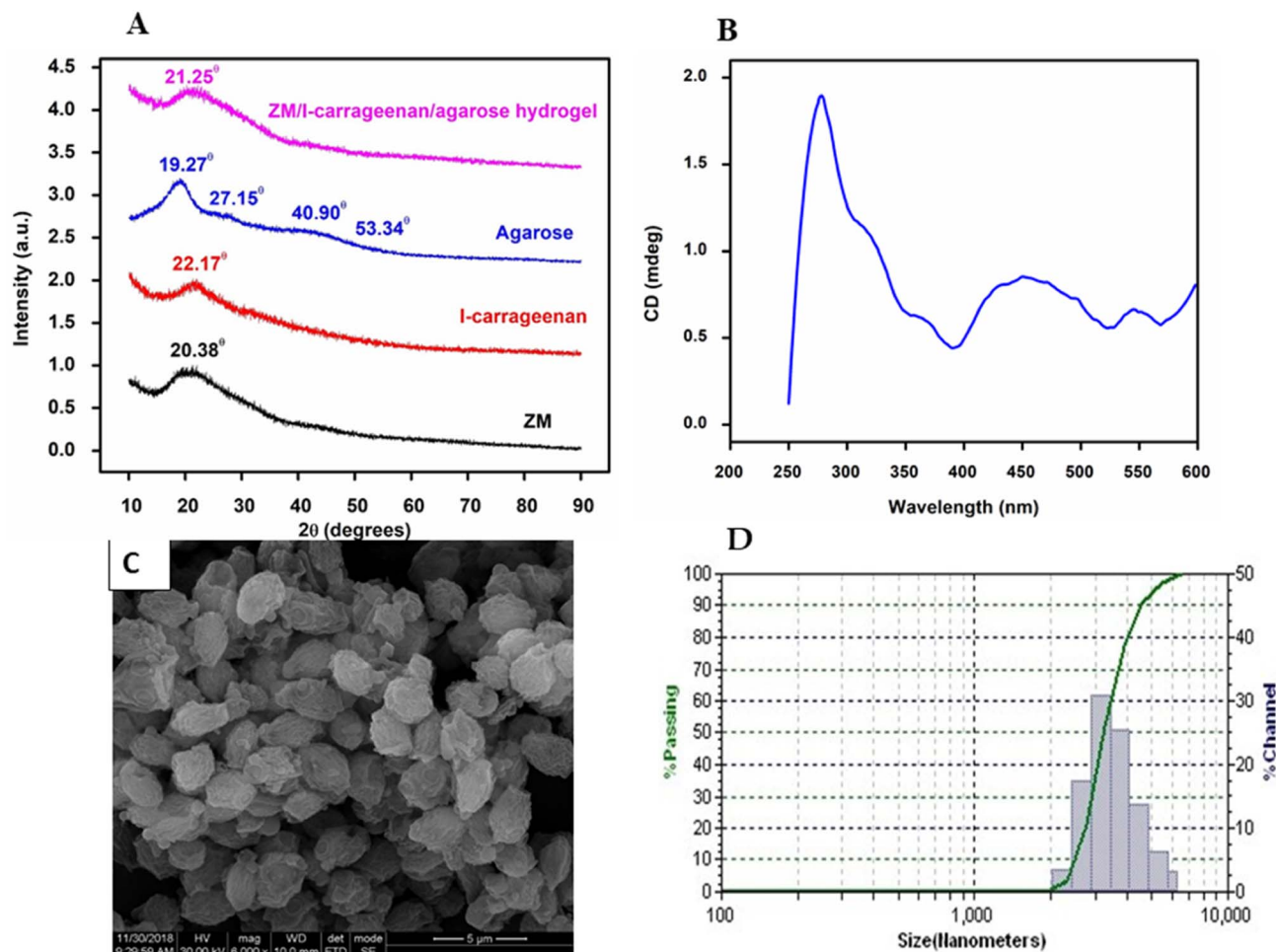


Fig. 1 (A) XRD of ZM, l-carrageenan, agarose and ZM/l-carrageenan/agarose gel. Strongest peak for ZM at  $20.38^\circ$  (represents crystalline nature of ZM), l-carrageenan broad peak at  $2\theta = 22.17^\circ$  (amorphous nature), agarose – crystalline peaks at  $19.27^\circ$ ,  $27.15^\circ$ ,  $40.90^\circ$ , and  $53.34^\circ$ , ZM/l-carrageenan/agarose gel – broad peak at  $21.25^\circ$  (amorphous nature). (B) CD spectra of ZM in aqueous solution. Helix-coil transition was observed at 320 nm and 450 nm in the visible region. (C) SEM image of ZM (scale bar 5  $\mu\text{m}$ ), (D) particle size distribution of ZM in aqueous solution (size of the particles 3.24 to 5.71  $\mu\text{m}$ ).

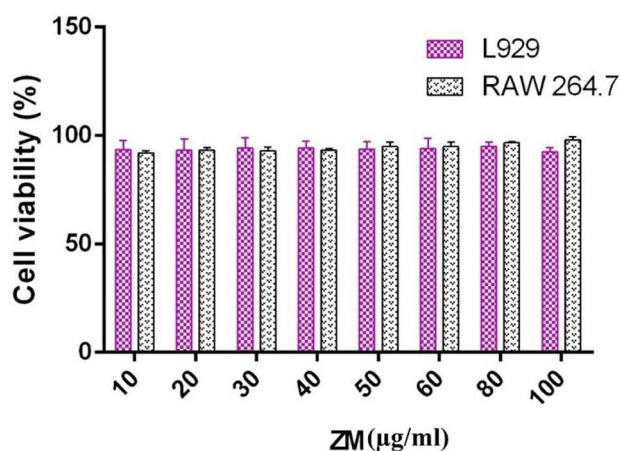


Fig. 2 Viability of L929 fibroblast and RAW 264.7 cell lines incubated with ZM. Cell viability was above 90% with both the cell lines, with no statistical significant difference.

### 3.3 ZM uptake by THP-1 differentiated macrophage and Raw 264.7 cells

After 4 h incubation with Rho B-tagged ZM, the cells were observed under fluorescence microscope and confocal microscope. ZM entered inside the cell which is observed as red colour particles (Fig. 3 and 4). The THP-1 differentiated macrophages are human phagocytic cells, the uptake of ZM by these cells could open up new therapeutic strategy to treat tumour associated macrophages and site directed drug delivery in cancer therapy. The Dectin-1 receptor of macrophage cells plays a major role in ZM uptake which acts as receptor. These glucans specifically binds with macrophages and enhances the innate immune responses by stimulating the cytokines and chemokines. The entry of these polysaccharides inside the macrophage is by phagocytosis *via* passive uptake through stearic or van der Waals interactions. High fluorescence intensity in the cells were quantified upon lysis which further indicates the Rho B-tagged ZM particle entry inside the cell. In our



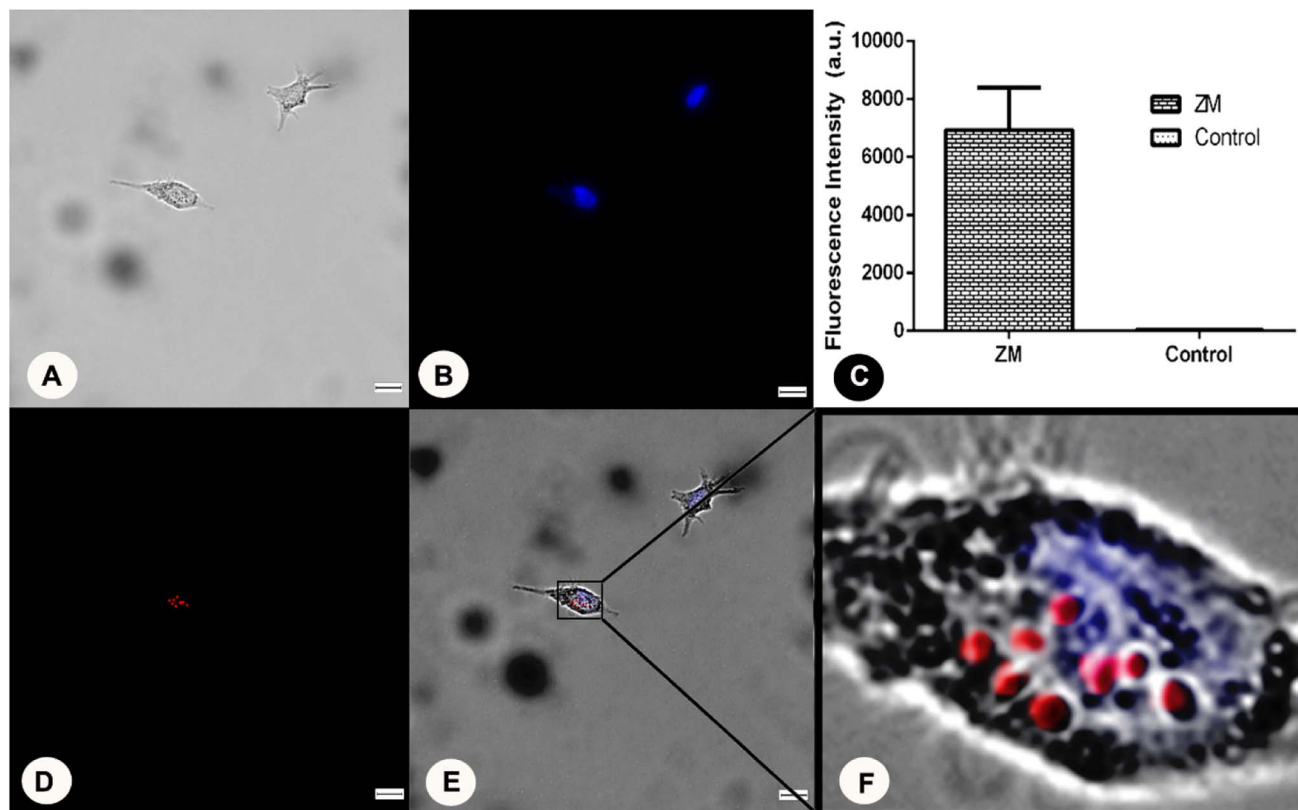


Fig. 3 Fluorescent microscopy images of differentiated THP-1 macrophages. (A) Bright field, (B) Dapi, (D) Rho B tagged ZM particles, (E) merged, (F) zoomed-in view of red colour ZM particles. Scale bar 20  $\mu\text{m}$ . (C) Fluorescent intensity of ZM, uptake by differentiated THP-1 macrophage cells.

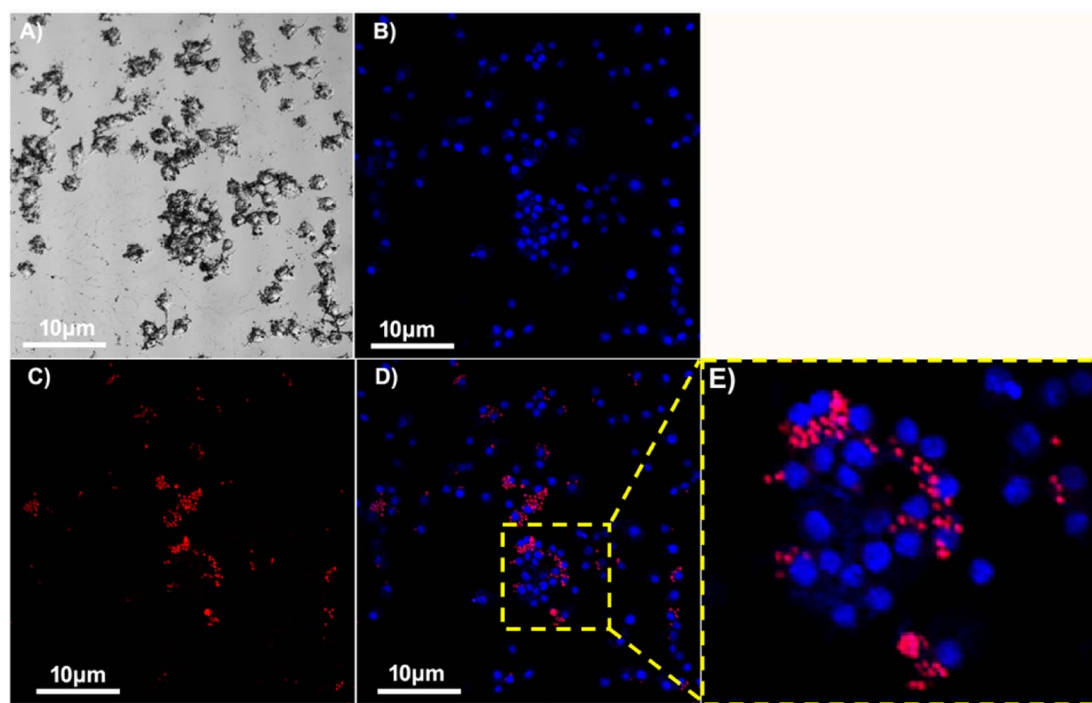


Fig. 4 Confocal images of Raw 264.7 macrophages tagged with Rho B tagged ZM particles. (A) Bright field (B) Dapi (C) Rho B (D) merged (E) zoomed-in view of red colour ZM particles. Scale bar 10  $\mu\text{m}$ .



previous study we have reported the ZM and ZMA uptake by Raw 264.7 cells which is mouse macrophage cell lines, but the present study concludes the polymer entry inside human differentiated THP-1 macrophages.

Raw 264.7 cells were grown in DMEM and checked for particle uptake, fortunately we were able to find the particle uptake by the cell directly and a video clip (Video 1:34 minutes) of the particle uptake was included in the ESI section (S3, Video abstract).<sup>†</sup> Direct particle uptake is a proof to confirm the Raw 264.7 cells surface receptors (Dectin 1) for ZM. ZM could be used for macrophage targeted drug delivery. Macropinocytosis occurs when particles >1  $\mu\text{m}$  enter the cell, similar to phagocytosis. Similar cell uptake results have been reported with curdlan and Dimethylaminoethyl (DMAEC) modified curdlan nanoparticles which are  $\beta$ -(1,3) glucan for SiRNA delivery to differentiated THP-1 cells. The mode of entry of DMAEC particles were found to be through Dectin-1 receptor present in Raw 264.7 and L929 fibroblast cells.<sup>11</sup> Raw 264.7 cells uptake of fluorescent probe based ZM inside cell was reported.<sup>17</sup> These results suggest a new mode of biomedical application in tumour models using glucans as carriers for delivering anti-cancer drugs and these biopolymers are not toxic but biocompatible.

*Dictyophora indusiate* (DIP) is a soluble  $\beta$ -D-glucan linked with  $\beta$ -(1,3)-(1,6)-side chain with a molecular weight of 650 kDa which binds with both Dectin-1 and TLR-4 receptors of macrophage exhibits anti-cancer activity. Further it has been proved to initiate the pathway of mitogen-activated protein kinase (MAPK), leads to NF- $\kappa$ B p65 phosphorylation, nuclear translocation and up-regulation of the secretion of IL-1 $\beta$  and TNF $\alpha$ .<sup>18</sup>

$\beta$ -(1,3)/(1,6)-Glucan from *Durvillaea antarctica* has shown protective effects on gastrointestinal cancer, especially on

colorectal cancer.  $\beta$ -(1,3)/(1,6)-glucan alone decreases the tumour in DLD1 xenograft and AOM-DSS stimulated tumour models. Glucan also enhances the antitumor effects of PD-1 antibody in syngeneic tumour model. Increased cytokine/chemokine secretion, macrophage phagocytosis and modulation of the systemic and intratumoral immune cell composition<sup>19</sup> was observed with  $\beta$ -(1,3)/(1,6)-glucan.

### 3.4 Competitive receptor blocking

Dectin-1 is the major receptor for polysaccharide entry into macrophage cells. Competitive receptor blocking experiment is carried out to determine whether the ZM particle entry is through Dectin-1 mediated endocytosis. Curdlan, has similar properties like ZM and is well known ligand for Dectin-1 receptor, same way other compounds were tested for different mode of entry which are, M- $\beta$ -CD (ligand for lipid mediated endocytosis, caveole (~ 60 nm)) and sucrose (Clathrin mediated endocytosis (~ 120 nm)). Among the three compounds tested curdlan showed ~1.6 fold of uptake inhibition (Fig. 5) at a concentration of 100  $\mu\text{g mL}^{-1}$ . M- $\beta$ -CD and sucrose did not show any difference in uptake efficiency. These results indicates ZM mode of entry to the cell is through Dectin-1 receptor mediated endocytosis.

### 3.5 M1, M2 and TLR-2 gene expression by ZM on differentiated THP-1 macrophage cells

M1, M2 and TLR-2 gene expression levels were quantified by real time PCR analysis. ZM were treated and tested for its expression levels of M1, M2 and TLR2 genes on differentiated THP-1 macrophage cell lines. The expression levels of M1 genes is upregulated with ZM treated cells, the TNF $\alpha$  fold change was  $4.99 \pm 1.00$  and  $8.64 \pm 1.0$  fold with CXCL10. Same way the M2

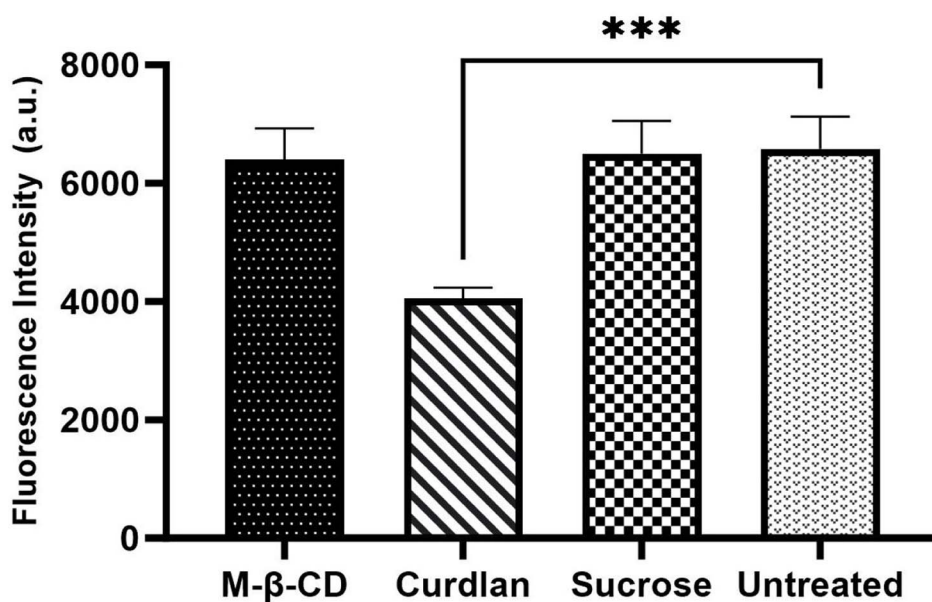


Fig. 5 Quantification of fluorescent intensity of Rho B tagged ZM particles uptake by Raw 264.7 (\*\*\*)  $p < 0.0005$ ) pre-treated with curdlan, M- $\beta$ -CD and sucrose separately.



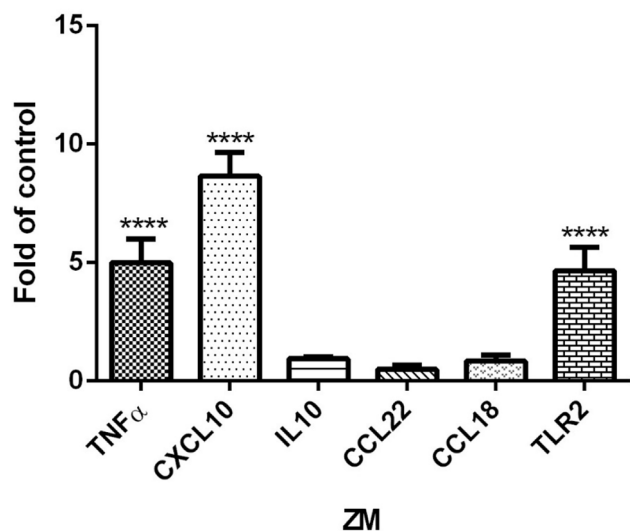


Fig. 6 Expression of M1 (TNF $\alpha$  and CXCL10), M2 (IL10, CCL22 and CCL18) and TLR 2 genes in differentiated THP-1 macrophages treated with ZM. \*\*\*\* $p < 0.0001$  with respect to the control (cells without the ZM and LPS treatment).

marker genes (IL10, CCL18 and CCL22) expression was decreased with a fold change of  $0.95 \pm 0.07$  in IL10,  $0.49 \pm 0.178$  with CCL22 and  $0.84 \pm 0.25$  with CCL18. Toll like receptor -2 gene expression was upregulated up to  $4.65 \pm 1.0$  fold with ZM treatment (Fig. 6). From the above results it is very clear that ZM upregulates M1 and TLR 2 genes and decrease the M2 expression levels thus aids its uses as drug carrier for targeting TAMs.

Recent study has shown that macrophages are major therapeutic targets for gene therapy. A biopolymer which targets the TAMs is necessary to treat granuloma in organs. M1 displays anti-tumoral functions which are generally considered as potent cells to kill microorganisms and tumour cells by producing pro-inflammatory cytokines. M2 shows protumoral functions includes inflammatory responses, scavenging debris, and matrix remodelling and tumour progression.<sup>3,11,16</sup> Curdlan from *Agrobacterium tumefaciens* sp. ATCC 31750 have been chemically modified with dimethylaminoethyl functional group to promote its gene binding ability which in turn upregulates the M1 marker genes (TNF $\alpha$  and CXCL10) and same time

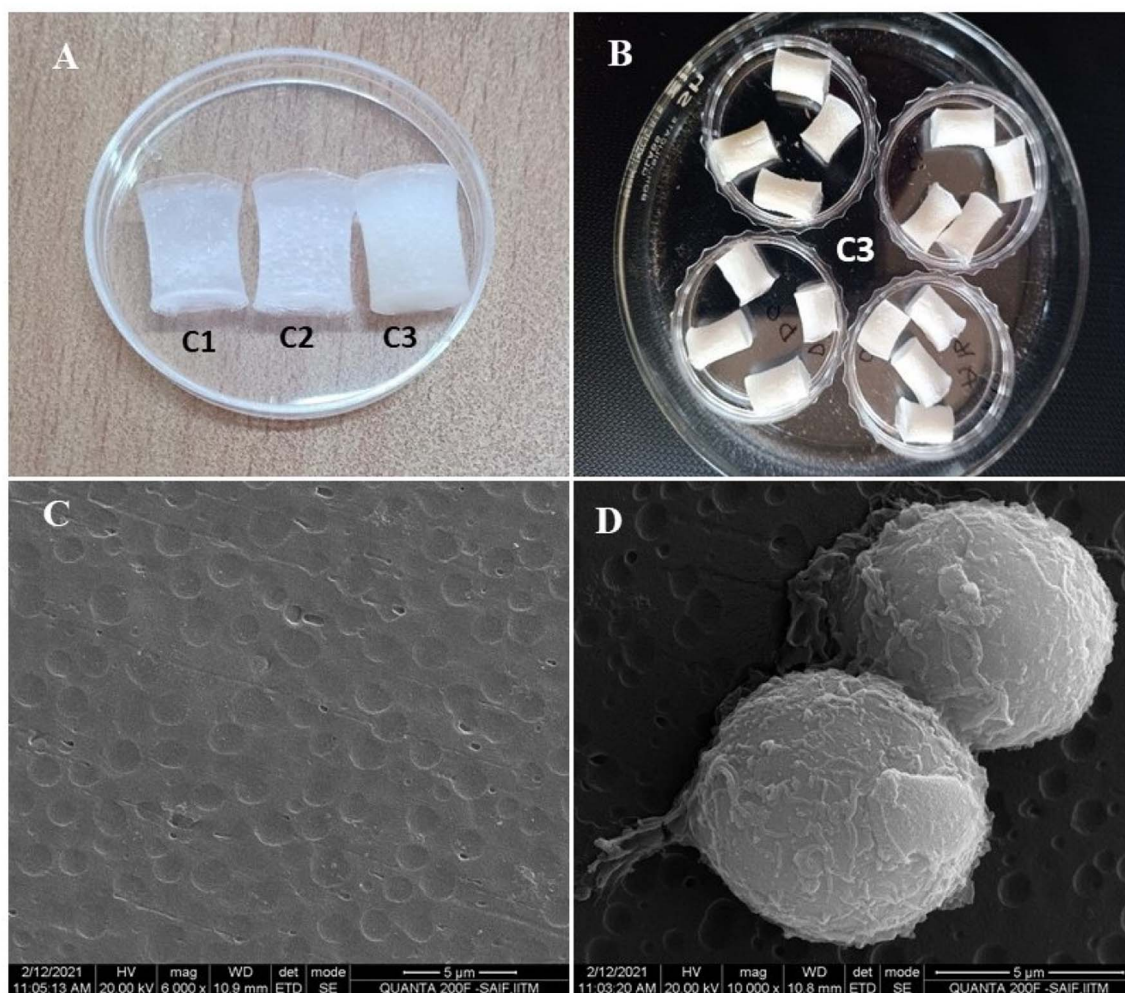


Fig. 7 (A) Wet hydrogel of ZM/l-carrageenan (three different ratios C1 (10 : 0), C2 (9 : 1), C3 (5 : 5)) and agarose (0.4%). (B) Freeze dried C3 ZM/l-carrageenan/agarose hydrogels appears as porous and spongy (11 mm in size), (C) SEM images of control ZM/l-carrageenan/agarose hydrogels (C3) without L929 cells. (D) L929 cells grown on ZM/l-carrageenan/agarose hydrogels (C3). Scale bar 5  $\mu\text{m}$ .





downregulates the levels of M2 marker genes (IL10, CCL18 and CCL22).

### 3.6 ZM/ $\iota$ -carrageenan/agarose hydrogel

Hydrogels were prepared with ZM/ $\iota$ -carrageenan/agarose. Different ratios of  $\iota$ -carrageenan from 0, 1 and 5 wt% up to a 5 : 5 were used for preparing the gel without chemical cross linkers. Among the three ratios tested C3 which had ZM/ $\iota$ -carrageenan (at 5 : 5) along with 0.4% agarose as gelling agent showed stable and rigid gel and not dispersed in cell culture medium. The prepared gels were soft, flexible, porous, spongy, and biocompatible and supported the growth of cells. After setting the hydrogels which are wet gels (Fig. 7A), were analyzed for their elasticity, stiffness, strength and pore size among them the C3 was chosen for further study which is lyophilized and porous gels were formed (Fig. 7B) which appears as oval shaped holes on the surface of the gel in SEM images of hydrogel (Fig. 7C). During lyophilization the water content of the hydrogel were removed and the gel appears spongy like networks and forms porous gel, further the gel were used for growing L929 cells. The hydrogel supported binding and attachment of L929 cells and they grow well on the hydrogel (Fig. 7D). Gels were fixed and viewed under a scanning electron microscope and they appeared as round shaped on the surface of the porous hydrogel. The zymosan/ $\iota$ -carrageenan/agarose

lyophilized hydrogel were analysed for polydispersity index (PDI) and Zeta potential. PDI is 6.80 and it shows the high polydispersity of the sample with multiple particle size populations. Zeta potential is 67.55 which indicates a more stable and colloidal nature of the gel. Stability of the zymosan/ $\iota$ -carrageenan/agarose hydrogel were analysed by immersing the gels in PBS, DMEM and RPMI media for different days (6 h to Day 3), and the gels were stable without any damage (Fig. 8).

To enhance the stability and insolubility in liquid medium the gel were mixed with agarose which was used as gelling agent. Agarose (derived from red algae) is biocompatible and a moisturizing polymer with mechanical properties like soft tissue and hence widely used as wound healing material.<sup>20–23</sup>  $\iota$ -Carrageenan structure has one additional sulfate group per two galactose unit which can increase its interactions with other cationic groups.<sup>2</sup> It also has strong gelation property and elastic nature and so widely used as biomaterial.  $\iota$ -Carrageenan (anionic) forms non-covalent and electrostatic interactions with cationic peptides and polysaccharides. As reported by others  $\iota$ -carrageenan<sup>24</sup> forms network with ZM and agarose. ZM/ $\iota$ -carrageenan/agarose are cross linked by intermolecular forces and ionic interactions.<sup>6</sup>  $\iota$ -Carrageenan possess hydroxyl and sulphate functional groups, ZM has hydroxyl groups which are finely cross linked by agarose fibrous networks.<sup>5</sup> It is reported that  $\kappa$ -carrageenan/agarose based hydrogels enriched with

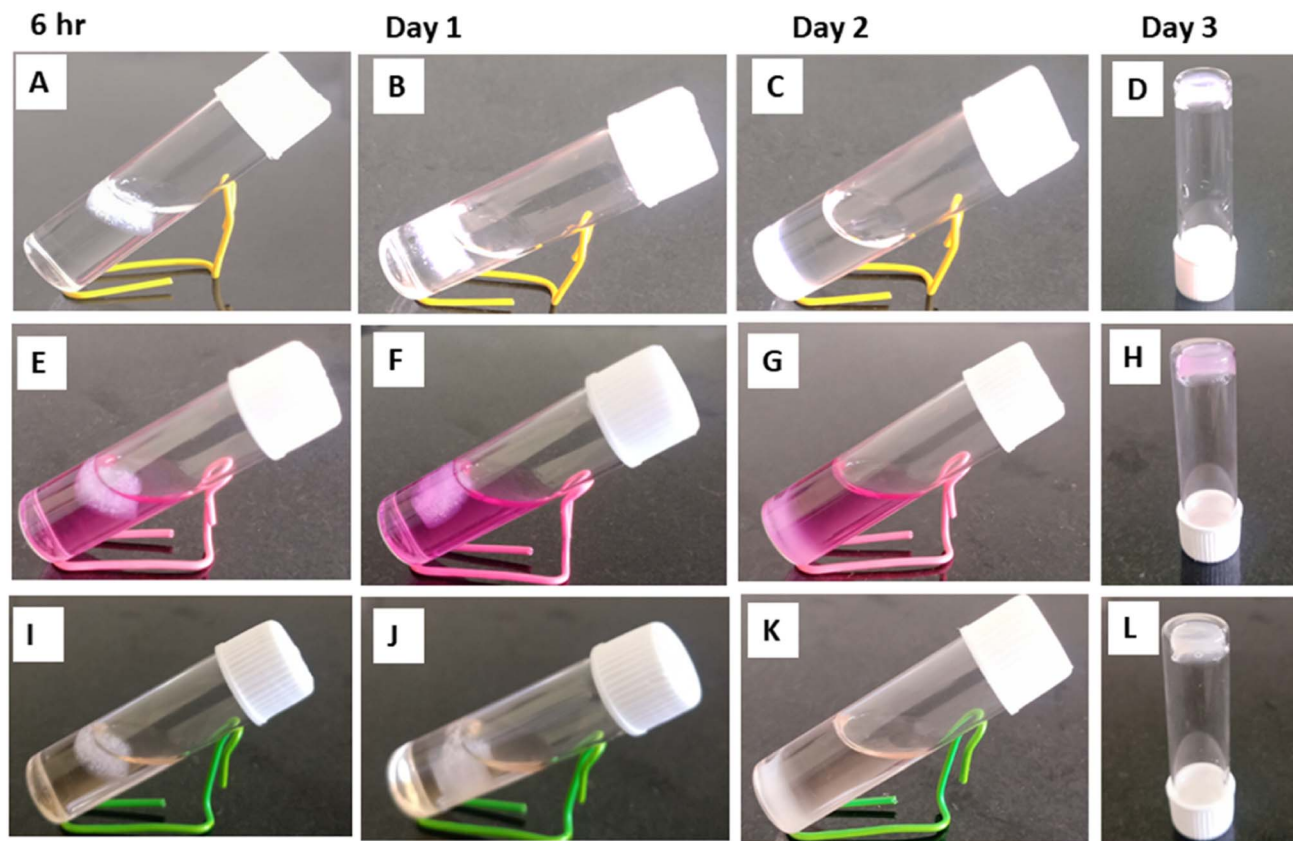


Fig. 8 Stability of the ZM/ $\iota$ -carrageenan/agarose hydrogel immersed in PBS, DMEM and RPMI media at different days. Hydrogel immersed in PBS (A) 6 h, (B) day 1, (C) day 2 (D) day 3. Hydrogel immersed in DMEM (E) 6 h, (F) day 1, (G) day 2, (H) day 3. Hydrogel immersed in RPMI (I) 6 h, (J) day 1, (K) day 2, (L) day 3.



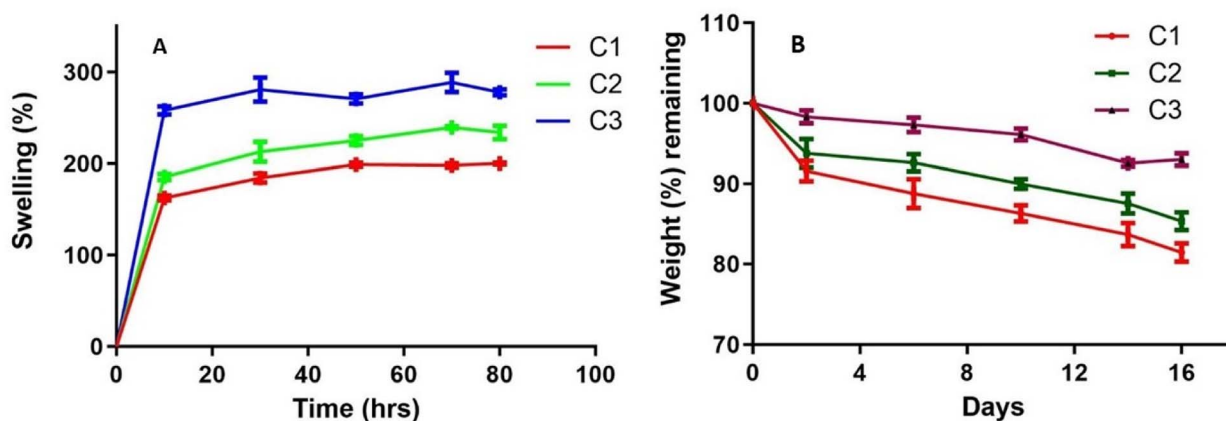


Fig. 9 Physicochemical properties of the Zymosan/ $\iota$ -carrageenan/agarose. ZM/ $\iota$ -carrageenan (three different ratios C1 (10 : 0), C2 (9 : 1), C3 (5 : 5)) and agarose (0.4%) used for swelling and degradation. (A) Swelling behavior in PBS (B) degradation study in PBS.

*Cryphaea heteromalla* (biophenols) aqueous extracts have been used for the treatment of cutaneous wound healing which reduces the excessive oxidative stress generation in the wound and enhance the healing process through the adhesion, migration and proliferation of 3T3 fibroblast cells.<sup>7</sup> The seaweed derived carrageenan is a versatile, promising biopolymer which enhances the extracellular matrix development and bone and cartilage tissue formation and act as potent wound healing biomaterial.

### 3.7 Swelling and biodegradation of the ZM/ $\iota$ -carrageenan/agarose hydrogel

ZM/ $\iota$ -carrageenan/agarose based wound dressing material is prepared to absorb the exudates and make them dry on the wounds, which prevents microbial infection and avoids the maceration of the wounded area. ZM is an excellent immunomodulator but shows the poor mechanical properties of a hydrogel. Adding  $\iota$ -carrageenan enhances the stability and could reduce intermolecular distance, which improves the density of the polymer network. ZM Along with  $\iota$ -carrageenan and agarose, improves the hydrogel's retention, loading, and protection properties. The hydrogels C1, C2, and C3 attain equilibrium after 24 h (Fig. 9A). The swelling percentage of C3 (ZM/ $\iota$ -carrageenan ratio 5 : 5) is  $\approx$  1.3 times higher than that of C1, which has a ZM/ $\iota$ -carrageenan ratio 10 : 0. The lower H<sub>2</sub>O uptake is observed with higher ZM concentrations, which is due to the poor mechanical and gelation properties. Moreover, the ZM is a highly branched glucan that has electron rich 'O' atoms in the OH groups, which hinder water uptake and decrease swelling properties.<sup>25</sup> Both hydrophilic and hydrophobic functional groups are present in ZM,  $\iota$ -carrageenan, and Agarose which are responsible for the swelling behaviour of the hydrogels.<sup>26</sup>

The wound healing materials are prepared to have slow degradation to maintain their properties and support tissue regeneration in the initial stage of wound healing. Fig. 9B shows the degradation pattern of the hydrogels. The initial degradation rate of the hydrogel is slower due to swelling. The C1

hydrogel suffered a weight loss of 18.5%, followed by the C2 hydrogel, which lost  $\approx$  14.67% after 16 days of immersion in PBS. The hydrolysis-resistant behaviour of ZM contributes to the slowdown of the degradation process, which is observed with curdlan, which has similar structural properties.<sup>27</sup> Whereas C3 suffered a weight loss of 7% due to the increased concentration of  $\iota$ -carrageenan when compared with C1 and C2. Literature reports have suggested that hydrogels which retain more water or exudates suffer higher degradation due to the penetration of water to the polymer matrix. Thus, higher swelling of the material leads to more water uptake of the hydrogel, which has an equal ratio of ZM and  $\iota$ -carrageenan and ends up with a higher degradation rate.<sup>28</sup>

## 4. Conclusion

Thermal and structural properties of ZM were evaluated, and the immunomodulatory effects, particularly the upregulation of M1, TLR-2 marker gene expressions of ZM on differentiated THP-1 macrophages was identified, these results shown that it specifically targets macrophages and activates into M1 (anti-tumoural) phenotype rather than M2 (pro-tumoural). It could be used as drug carrier for TAMs. ZM is biocompatible, nontoxic to L929 and RAW 264.7 cells even at the concentration of 100  $\mu$ g mL<sup>-1</sup>.  $\iota$ -Carrageenan and agarose were used for making hydrogels along with ZM, which support the attachment and growth of L929 cells which will be used as wound healing material. ZM had multifarious applications as drug carrier for TAMs and also as wound healing material.

## Author contributions

Geetha Venkatachalam – conceived and designed the experiments; performed the experiments; wrote the paper. Jayant Giri – investigation. Saurav Mallik – investigation. Zhongming Zhao – investigation. Gandarvakottai Senthilkumar Arumugam – methodology, validation of chemical structure. Manavalan Arulmani – Microscopic imaging analysis, Vimal Kumar

Dewangan – validation, imaging. Mukesh Doble – supervision, review and editing.

## Conflicts of interest

The authors declare no competing financial interest.

## Acknowledgements

The authors thanks the Department of Biotechnology and Sophisticated Analytical Instrument Facility (SAIF), IIT-Madras for analytical help. We thank Prof. Sathyanarayana Gummadi, IIT-madras for the timely help in the X-ray diffraction analysis.

## References

- G. Venkatachalam, S. Arumugam and M. Doble, Synthesis, Characterization, and Biological Activity of Aminated Zymosan, *ACS Omega*, 2020, 5, 15973–15982.
- B. Muszyńska, A. Grzywacz-Kisielewska, K. Kała and J. Gdula-Argasińska, Anti-inflammatory properties of edible mushrooms: A review, *Food Chem.*, 2018, 243, 373–381.
- A. Sica, T. Schioppa, A. Mantovani and P. Allavena, Tumour-associated macrophages are a distinct M2 polarised population promoting tumour progression: Potential targets of anti-cancer therapy, *Euro. J. Cancer*, 2006, 42, 717–727.
- G. Genard, S. Lucas and C. Michiels, Reprogramming of tumor associated macrophages with anticancer therapies: radiotherapy versus chemo- and immunotherapies, *Front. Immunol.*, 2017, 8, 1–19.
- V. L. Campo, D. F. Kawano, D. B. da Silva and D. B. Carvalho, Carrageenans: Biological properties, chemical modifications and structural analysis – A review, *Carbohydr. Polym.*, 2009, 77, 167–180.
- R. Yegappan, V. Selvaprithiviraj, S. Amirthalingam and R. Jayakumar, Carrageenan based hydrogels for drug delivery, tissue engineering and wound healing, *Carbohydr. Polym.*, 2018, 198, 385–400.
- L. A. Ditta, E. Rao, F. Provenzano, J. L. Sánchez, R. Santonocito, R. Passantino, M. A. Costa, A. Sabatino, D. Giacomazza, P. L. San Biagio, R. Lapasin and C. Dispenza, Agarose/ $\kappa$ -carrageenan-based hydrogel film enriched with natural plant extracts for the treatment of cutaneous wounds, *Int. J. Biol. Macromol.*, 2020, 164, 2818–2830.
- S. Latiyan, T. S. Sampath Kumar and M. Doble, Fabrication and evaluation of multifunctional agarose based electrospun scaffolds for cutaneous wound repairs, *J. Tissue Eng. Regen. Med.*, 2022, 16, 653–664.
- K. Ogawa and M. Hatano, Circular dichroism of the complex of a (1-3)- $\beta$ -D-glucan with Congo red, *Carbohydr. Res.*, 1978, 67, 527–535.
- M. Nováka, A. Synytsyaa, O. Gedeonb, *et al.*, Yeast (1-3),(1-6)-D-glucan films: Preparation and characterization of some structural and physical properties, *Carbohydr. Polym.*, 2012, 87, 2496–2504.
- Y. R. Basha, G. Venkatachalam, T. S. Sampath Kumar and M. Doble, Dimethylaminoethyl modified curdlan nanoparticles for targeted siRNA delivery to macrophages, *Mater. Sci. Eng., C*, 2020, 108, 110379.
- M. Salgado, S. Rodríguez-Rojo, R. L. Rei, M. J. Cocero and A. R. C. Duarte, Preparation of barley and yeast  $\beta$ -glucan scaffolds by hydrogel foaming: Evaluation of dexamethasone release, *J. Supercrit. Fluids*, 2017, 127, 158–165.
- X. Qi, T. Su, M. Zhang, X. Tong, W. Pan, Q. Zeng, Z. Zhou, L. Shen, X. He and J. Shen, Macroporous Hydrogel Scaffolds with Tunable Physicochemical Properties for Tissue Engineering Constructed Using Renewable Polysaccharides, *ACS Appl. Mater. Interfaces*, 2020, 12, 13256–13264.
- H. Saito, T. Ohki and T. Sasaki, A  $^{13}\text{C}$ -nuclear magnetic resonance study of gel-forming (1-3)- $\beta$ -D-glucans. Evidence of the presence of single-helical confirmation in a resilient gel of a curdlan-type polysaccharide 13140, *Biochemistry*, 1977, 16, 908–914.
- A. Javmen, A. Nemeikaitė-Čėnienė, S. Grigėškis, J. Lysovienė, I. Jonauskienė and A. Š. M. Mauricas, The effect of *Saccharomyces cerevisiae*  $\beta$ -glucan on proliferation, phagocytosis and cytokine production of murine macrophages and dendritic cells, *Biologia*, 2017, 72, 561–568.
- A. Su, M. Lu, T. Lu, M. N. Lai and L. TeikNg, (1 $\rightarrow$ 6)-Branched (1 $\rightarrow$ 4)- $\beta$ -D-Glucan from *Grifola frondosa* Inhibits Lipopolysaccharide-Induced Cytokine Production in RAW264.7 Macrophages by Binding to TLR2 Rather than Dectin-1 or CR3 Receptors, *J. Nat. Prod.*, 2020, 83, 231–242.
- J. Park, H. Kim, Y. Choi and Y. Kim, A Ratiometric Fluorescent Probe Based on a BODIPY-DCDHF Conjugate for the Detection of Hypochlorous Acid in Living Cells, *Analyst*, 2013, 138, 3368–3371.
- F. Su, Q. Song, C. Zhang, X. Xu, M. Li, D. Yao, L. Wu, X. Qu, H. Guan, G. Yu, J. Yang and C. Zhao, A beta-1,3/1,6-glucan from *durvillaea Antarctica* inhibits tumor progression *in vivo* as an immune stimulator, *Carbohydr. Polym.*, 2019, 222, 114993.
- C. Deng, H. Fu, J. Shang, J. Chen and X. Xu, Dectin-1 mediates the immunoenhancement effect of the polysaccharide from *dictyophora indusiata*, *Int. J. Biol. Macromol.*, 2018, 109, 369–374.
- X. Bao, K. Hayashi, Y. Li, A. Teramoto and K. Abe, Novel agarose and agar fibers: Fabrication and characterization, *Mater. Lett.*, 2010, 64, 2435–2437.
- S. Sakai, K. Kawabata, T. Ono, H. Ijima and K. Kawakami, Development of mammalian cell-enclosing subsieve-size agarose capsules (<100 microm) for cell therapy, *Biomaterials*, 2005, 26, 4786–4792.
- N. Ninan, A. Forget, V. P. Shastri, N. H. Voelcker and A. Blencowe, Antibacterial and Anti-Inflammatory pH-Responsive Tannic Acid-Carboxylated Agarose Composite Hydrogels for Wound Healing, *ACS Appl. Mater. Interfaces*, 2016, 8, 28511–28521.



- 23 Z. Noralian, M. P. Gashti, M. R. Moghaddam, H. Tayyeb and I. Erfanian, Ultrasonically developed silver/iota-carrageenan/cotton bionanocomposite as an efficient material for biomedical applications, *Int. J. Biol. Macromol.*, 2021, **180**, 439–457.
- 24 S. Girod, M. Boissière, K. Longchambon, S. Begu, C. Tourne-Pétheil and J. M. Devoisselle, Polyelectrolyte complex formation between iota-carrageenan and poly (l-lysine) in dilute aqueous solutions: a spectroscopic and conformational study, *Carbohydr. Polym.*, 2004, **55**, 37–45.
- 25 S. Agnihotri, S. Mukherji and S. Mukherji, Antimicrobial chitosan–PVA hydrogel as a nanoreactor and immobilizing matrix for silver nanoparticles, *Appl. Nanosci.*, 2012, **2**, 179.
- 26 S. Latiyan, T. S. Sampath Kumar and M. Doble, Fabrication and evaluation of agarose-curdlan blend derived multifunctional nanofibrous mats for diabetic wounds, *Int. J. Biol. Macromol.*, 2023, **235**, 123904.
- 27 C. Grandpierre, H. G. Janssen, C. Laroche, P. Michaud and J. Warrand, Enzymatic and chemical degradation of curdlan targeting the production of  $\beta$ -(1  $\rightarrow$  3). oligoglucans, *Carbohydr. Polym.*, 2008, **71**, 277–286.
- 28 S. Rafeian, H. Mahdavi and M. E. Masoumi, Improved mechanical, physical and biological properties of chitosan films using Aloe vera and electrospun PVA nanofibers for wound dressing applications, *J. Ind. Text.*, 2021, **50**, 1456–1474.

